

PACS numbers: 42.40.Kw; 42.87.Bg
DOI: 10.1070/QE2005v035n02ABEH002641

Aberration-free holographic reverse-shearing interferometry

A.M. Lyalikov

***Abstract*. The peculiarities of holographic reverse-shearing interferometry, which make it possible to obtain two simultaneous real-time interferograms of the phase object free from aberrations of the optical system are studied. The behaviour of fringes in the interferograms is identical to their behaviour in the conventional two-beam interferometry with a standard reference wave. The peculiarities of fringe alignment in the interferograms are considered. The real-time interferograms of a glass test plate with various fringe alignments are obtained, confirming the practical prospects of this technique.**

Keywords: *phase object, wave front, interference pattern, hologram.*

1. Introduction

The application of the classical interferometric methods [1, 2] based on the principle of distorted wave front comparison with the reference wave front is quite complicated in a number of cases. This is due mainly to the problems related to the formation of the reference wave. Such problems arise in determining the shape of the wave front of a single light beam emitted by a laser or a light beam propagated through the perturbing atmospheric fields [3, 4]. Under these conditions one has to resort to the wave front investigation techniques in which the reference wave is either absent or formed by the object wave. Such methods include the shadow technique for studying the wave front using different beam-limiting apertures [5 – 7], interferometry with a local reference wave or diffraction from a point [6, 8, 9] and shearing interferometry [6, 10, 11].

Shearing interferometry is attractive in view of the relative simplicity of its optical scheme and high vibration stability of the interferometers themselves, and is widely used in various fields of science and technology [9 – 15].

Apart from the lateral-shearing interferometry which is used most frequently, rotational- and reverse-shearing interferometry has also found practical applications in some cases [6, 16]. The use of holography principles for obtaining interferograms with various kinds of shears allowed a compensation of the optical system aberrations during real-time investigations [17, 18]. It was proposed in papers [19, 20] to produce the reverse shear both in longitudinal and radial directions. In the radial-shearing holographic interferometry, a Gabor zone plate was used for these purposes [21 – 23].

The main specific feature of shearing interferometry is the dependence of interference fringes both on the type of shear of interfering wave fronts and on its magnitude. However, if the phase object under study occupies a part of the working field and its size is smaller than the shear value, the interference fringes are identical to those obtained in two-beam, reference-wave interferometry [24]. This particular case of shearing interferometry deserves special attention because it combines simultaneously all the advantages of both the methods mentioned above and eliminates the complexity of deciphering the interferograms, which are inherent in shearing interferometry. The diameters of separated interfering light beams are identical for typical schemes used for obtaining lateral-, rotational- and reverse-shearing interferograms [6, 25, 26]. Obviously, the particular case mentioned above can be realised in such schemes only if the size of the investigated object does not exceed half the diameter of the light beam.

Figure 1 shows the geometrical images of the contours of interfering light beams in the case of lateral-shearing interferometry for the shear Δs equal to half the beam diameter, as well as for the reverse shear. Here, we have considered cases of the maximal size of the phase object. The latter is shown in Fig. 1 as a triangle. The width of this object in the direction of the shear (i.e., in the x direction) does not exceed half the light beam diameter. For lateral-shearing interferometry (Fig. 1a), the maximum shear Δs along the x axis is equal to half the beam diameter. The hatched areas correspond to the regions of formation of interferograms due to superimposition of the part of the beam transmitted through the object on the part of the beam not distorted by the object. The reverse- or rotational-shearing interferometry upon the rotation of one of the beams through 180° (Figs 1a and b) is preferable to the lateral-shearing interferometry. This advantage is manifested at least in a 1.3-fold increase in the useful area of the overlap of separated light beams where the interference pattern visualising the investigated phase object is observed.

In this paper, we consider the peculiarities of the holographic version of the reverse-shearing interferometry which allows us to obtain aberration-free, real-time interferograms of the phase object with an arbitrary alignment of the fringes whose behaviour is identical to their behaviour in a conventional two-beam reference-wave interferometry. Note that this method of reverse-shearing interferometry

A.M. Lyalikov Yanka Kupala Grodno State University, ul. Ozheshko 22, Grodno, 230023 Belarus, e-mail: lyalikov@inbox.ru

Received 11 March 2004; revision received 6 October 2004
Kvantovaya Elektronika **35** (2) 191 – 194 (2005)
Translated by Ram Wadhwa

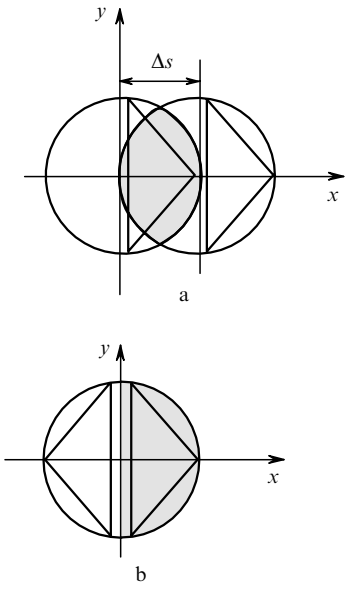

Figure 1. Images of the contours of interfering beams obtained in lateral- (a) and reverse-shearing (b) interferometry.

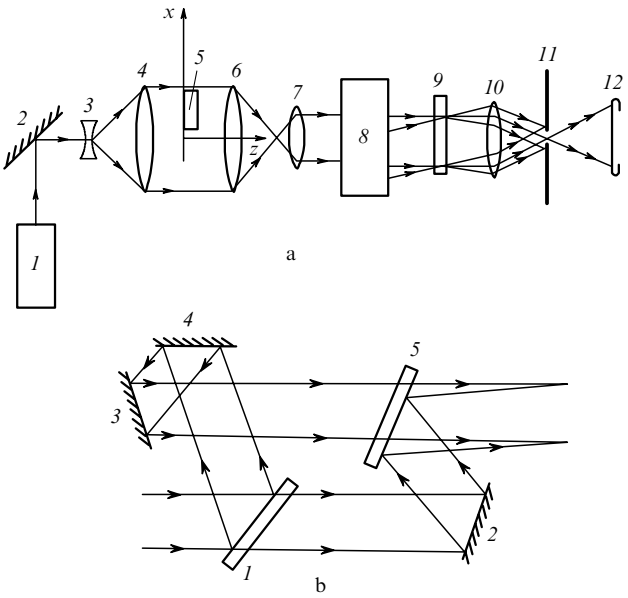

Figure 2. Optical schemes of the experimental setup (a) and a reverse-shearing interferometer (b): (a) (*1*) He–Ne laser; (*2*) mirror; (*3*), (*4*) and (*6*), (*7*) telescopic systems; (*5*) phase object under study; (*8*) reverse-shearing interferometer; (*9*) hologram (plane of the hologram); (*10*) objective; (*11*) selective aperture; (*12*) plane of interferogram recording; (b) (*1*), (*5*) beamsplitters; (*2*)–(*4*) reflecting mirrors.

is applicable only for studying phase objects whose size does not exceed half the diameter of the probe light beam, and for the case of complete compensation for the optical-scheme aberrations.

2. Experimental setup

Figure 2a shows the optical scheme (view from top) of the setup used for holographic reverse-shearing interferometry. The radiation from He–Ne laser (*1*) was directed by mirror (*2*) to a telescopic system formed by concave lens (*3*) and objective (*4*). This optical system formed a collimated light beam of required dimensions for illuminating phase object (*5*). The second telescopic system formed by objectives (*6*) and (*7*) reduced the diameter of the object light beam. The phase object was placed between objectives (*4*) and (*6*), its size not exceeding half the diameter of the light beam. The light beam from the object was directed to reverse-shearing interferometer (*8*).

Figure 2b shows the optical scheme (view from top) of the reverse-shearing interferometer used in experiments. Beamsplitter (*1*) divided the object light beam into two beams which were directed by mirrors (*2*) (the first beam) and (*4*), (*3*) (the second beam) to second beamsplitter (*5*). The second light beam propagating along interferometer arm (*1*), (*4*), (*3*) and (*5*) was turned by 180° around the z axis. Only the direction of the x axis was reversed in this case, while the direction of the y axis relative to the second beam remained unchanged. The angle between the interfering beams was set by rotating mirror (*2*) and beamsplitter (*5*).

Light beams were made to coincide in the plane of hologram (*9*) (Fig. 2a). Hologram (*9*) was recorded without phase object (*5*). The aberrations of the optical scheme recorded on this hologram were then eliminated at the stage of obtaining interferograms in plane (*12*). The planes of the interferogram and the object under study were aligned optically with the help of objectives (*6*), (*7*) and (*10*). Diaphragm (*11*) placed at the back focal plane of objective (*10*) separated the required number of light-diffraction orders on hologram (*9*).

Note that an IAB-451 shadow instrument [9] or the object arm of any laser interferometer with a narrow reference beam (for example, IZK-463 with a field of view of 800 mm) can be used for elements (*3*), (*4*), (*6*) and (*7*) in the optical scheme of the setup. In the latter case, the technique described above can be used to investigate phase objects of size up to 400 mm.

3. Hologram recording

The aberrations of the optical system were recorded on hologram (*9*) (Fig. 2a) before placing phase object (*5*) into the probe beam. We used a system of coordinates x, y, z in which the light beam propagating through the object under study was directed along the z axis coinciding with the principal optical axis of the system, while the reverse shear was performed in interferometer (*8*) by reversing only the direction of the x axis of one of the light beams. We assume that the optical scheme of the reverse-shearing interferometer (Fig. 2b) is aligned so that the first light beam is inclined in the xz plane to the x axis at a certain angle α_0, while the second beam experiences reverse shear and propagates along the z axis. In this case, the complex beam amplitudes at the output of the interferometer can be written in the form

$$A_{01}(x,y) = a_1 \exp\{\mathrm{i}[2\pi\xi_0 x + \varepsilon_0(x,y) + \varepsilon_1(x,y)]\}, \qquad (1)$$

$$A_{02}(x,y) = a_2 \exp\{\mathrm{i}[\varepsilon_0(-x,y) + \varepsilon_2(x,y)]\}, \qquad (2)$$

where a_1 and a_2 are the real amplitudes; $\xi_0 = \cos\alpha_0/\lambda$ is the spatial frequency of the wave; λ is the wavelength; ε_0 are the phase distortions introduced by aberrations of the object

arm of the optical system; $\varepsilon_1(x, y)$ and $\varepsilon_2(x, y)$ are the phase distortions introduced by aberrations of the first and second arm of the reverse-shearing interferometer. Thus, a hologram is recorded in plane (*9*). If the linear recording conditions are fulfilled and it is assumed that $a_1 = a_2$, the amplitude transmission of the hologram is

$$\tau(x, y) = 1 + \cos[2\pi\xi_0 x + \varepsilon_0(x, y) - \varepsilon_0(-x, y) + \varepsilon_1(x, y) - \varepsilon_2(x, y)]. \quad (3)$$

After chemical processing of the hologram, it is placed at its original position (*9*).

4. Real-time recording of interferograms

Phase object (*5*) under study (Fig. 2a) was placed between objectives (*4*) and (*6*) in such a way that its size along the x axis did not exceed half the diameter of the light beam. For example, the object may be placed in the I and IV quadrants of the xy coordinate system. This is a necessary condition for realising the technique described here. In the reverse-shearing interferometer (Fig. 2b), interferograms with any alignment of fringes can be obtained in real time by changing the direction of propagation of the first beam with respect to the x and y axes by small angles α and β respectively relative to α_0. Hologram (*9*) is illuminated by two light beams. Diaphragm (*11*) is used to separate the wave passing directly through hologram (*9*) and the wave diffracted in first order. In this case, the interference pattern produced in plane (*12*) is described by the expression

$$I_1(x, y) = 1 + \frac{2b_1 b_2}{b_1^2 + b_2^2}\cos\{2\pi\xi x + 2\pi\eta y + [\varphi(x, y) - \varphi(-x, y)]\}, \quad (4)$$

where b_1 and b_2 are the real amplitudes of the interfering waves; $\xi = \cos\alpha/\lambda$; $\eta = \cos\beta/\lambda$; and $\varphi(x, y)$ is the phase variation caused by the phase object under study.

One can see from expression (4) that the real-time interference pattern is free from aberrations $\varepsilon_0(x, y)$, $\varepsilon_1(x, y)$ and $\varepsilon_2(x, y)$ of the optical system [9, 26]. Figure 3 shows the reverse-shearing interferogram aligned to an infinitely broad fringe, which was obtained in plane (*9*) in the absence of object (*5*). This interferogram characterises the distortions of the interference fringes due to aberrations resulting from the action of the sum of functions $\varepsilon_0(x, y) - \varepsilon_0(-x, y) + \varepsilon_1(x, y) - \varepsilon_2(x, y)$ according to (3).

Interference pattern (4) has a remarkable singularity. Because the size of the object under study along the x axis does not exceed half the diameter of the light beam, i.e., the object lies in the I and IV quadrants of the xy coordinate system, function $\varphi(x, y)$ vanishes at points lying in the II and III quadrants. Accordingly, function $\varphi(-x, y)$ vanishes at points lying in the I and IV quadrants. For this reason, the interference patterns visualising the behaviour of the functions $\varphi(x, y)$ and $\varphi(-x, y)$ will be separated in observation plane (*12*) (Fig. 2a) and will lie in the I, IV and II, III quadrants, respectively. We will arbitrary call these interference patterns right and left interferograms, respectively.

In this case, the fringe equations for the right and left interferograms will have the form:

$$2\pi\xi x + 2\pi\eta y + \varphi(x, y) = 2\pi N, \quad (5)$$

Figure 3. Reverse-shearing interferogram characterising the aberration of the experimental setup.

$$2\pi\xi x + 2\pi\eta y - \varphi(-x, y) = 2\pi N, \quad (6)$$

respectively, where $N = 0, \pm 1, \pm 2, \ldots$. One can see from (5) and (6) that these interferograms do not differ in principle from the two-beam interferograms with a standard reference wave.

Figure 4 shows a series of real-time interferograms for a glass test plate. The vertical edge of the plate is parallel to the y axis. The plate occupies less than half the region of the object beam, providing the creation of a region in the vicinity of the unperturbed object having the shape of a vertical strip and dividing the interferogram into the left and right interferograms. The alignment of the interference fringes is also visualised in this vertical strip.

Consider the particular cases of the alignment of interference fringes for the left and right interferograms.

Alignment to an infinitely broad fringe corresponds to $\xi = \eta = 0$. In this case, expressions (5) and (6) for the left and right interferograms will take the form:

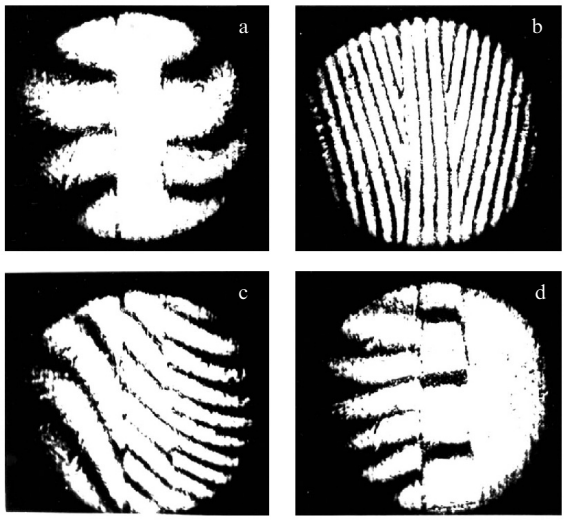

Figure 4. Interferograms of a glass test plate with different alignments of the fringes.

$$\varphi(x, y) - 2\pi N = 0, \quad (7)$$

$$\varphi(-x, y) - 2\pi N = 0, \quad (8)$$

respectively. The interference fringes described by the families of curves (7) and (8) are symmetric relative to the y axis.

Symmetry of the interference fringes relative to the y axis is also observed for an exact alignment to the vertical fringes ($\eta = 0$). In this case, the fringe equations for the right and left interferograms have the form

$$\varphi(x, y) + 2\pi\xi x - 2\pi N = 0, \quad (9)$$

$$\varphi(-x, y) - 2\pi\xi x - 2\pi N = 0. \quad (10)$$

Figures 4a and b show the photographs of the interference patters for a glass test plate aligned to an infinitely broad fringe (Fig. 4a) and a vertical fringe (Fig. 4b).

Symmetry of the interference fringes for the right (5) and left (6) interferograms relative to the y axis will be violated for any other alignment. This is confirmed by the photographs of the interference patterns presented in Figs 4c and d. In the presence of uncompensated aberrations, however, the above symmetry will also be violated for alignment to an infinitely broad fringe and a vertical fringe.

5. Conclusions

Thus, if the transverse dimensions of the phase object under study do not exceed half the probe beam diameter, the holographic reverse-shearing interference technique makes it possible to obtain real-time aberration-free interferogram in the form of a pair of interferograms visualising the phase object. The nature of fringes in these interferograms does not differ from those obtained by two-beam reference-wave interferometry.

The symmetric nature of the right- and left interferograms upon alignment to an infinitely broad fringe and a vertical fringe can be used for adjustments required in the case of a more precise alignment of the interferograms. The processing of each of the interferogram followed by the averaging of the results reduces the error in determining the function $\varphi(x, y)$.

The violation of symmetry of the fringes for other alignments can be used for increasing the information content of measurements, i.e., for a simultaneous real-time recording of two interferograms with different behaviours of fringes in the region of optical inhomogeneity.

References

1. Kolomiitsov Yu.V. *Interferometriya* (Interferometry) (Leningrad: Nauka, 1977).
2. Nagibina I.M. *Interferentsiya i diffraktsiya sveta* (Interference and Diffraction of Light) (Leningrad: Mashinostroenie, 1985).
3. Vorontsov M.A., Koryabin A.V., Shmal'gauzen V.I. *Upravlyaemye opticheskie sistemy* (Controlled Optical Systems) (Moscow: Nauka, 1988).
4. Luk'yanov D.P., Kornienko A.A., Rudnitskii B.E. *Opticheskie adaptivniye sistemy* (Adaptive Optical Systems) (Moscow: Radio i Svyaz', 1989).
5. Vasil'ev L.A. *Teneviye metody* (Shadow Techniques) (Moscow: Nauka, 1968).
6. Malakara D. (Ed.) *Opticheskii proizvodstvenniy kontrol* (Optical Production Control) (Moscow: Mashinostroenie, 1985).
7. Andreev A.I., Dukhopel I.I., Chunin B.A. *Opt-mekh. prom.*, **11**, 49 (1990).
8. Ivanov I.P., Tsvetkov A.D. *Kvantovaya Eelektron.*, **21**, 389 (1994) [*Quantum Electron.*, **24**, 363 (1994)].
9. Beketova A.K., Belozerov A.F., Berezkin A.N., et al. *Gologaficheskaya interferometrya fazovykh ob'ektov* (Holographic Interferometry of Phase Objects) (Leningrad: Nauka, 1979).
10. Nugumanov A.N., Smironov R.V., Sokolov V.I. *Kvantovaya Elektron.*, **30**, 435 (2000) [*Quantum Elektron.*, **30**, 435 (2000)].
11. Sokolov V.I. *Kvantovaya Elektron.*, **31**, 891 (2001) [*Quantum Electron.*, 31, 891 (2001)].
12. Schwider J. *Optik*, **108**, 181 (1998).
13. Ivanov P.V., Koryabin A.V., Shmal'gauzen V.I. *Kvantovaya Elektron.*, **27**, 78 (1999) [*Quantum Electron.*, **29**, 360 (1999)].
14. Santhanakrishnan T., Palanisamy P.K., Sirohi R.S. *Appl. Opt.*, **37**, 3447 (1998).
15. Bashkin A.S., Korotkov P.I., Maksimov Yu.P. *Kvantovaya Elektron.*, **24**, 786 (1997) [*Quantum Electron.*, **27**, 766 (1997)].
16. Saunders J.B. *J. Res. National Bur. Stand. B*, **66**, 29 (1962).
17. Bryngdahl O. *J. Opt. Soc. Am.*, **58**, 865 (1968).
18. Kulkarni V.G. *Opt. Laser Technol.*, **11**, 269 (1979).
19. Bryngdahl O. *J. Opt. Soc. Am.*, **59**, 142 (1969).
20. Bryngdahl O. *J. Opt. Soc. Am.*, **60**, 915 (1970).
21. Fouere J.C., Roychoudhuri C. *Opt. Commun.*, **12**, 29 (1974).
22. Fouere J.C., Malacara D. *Appl. Opt.*, **13**, 2035 (1974).
23. Fouere J.C. *Opt. Laser Technol.*, **6**, 181 (1974).
24. Komisssaruk V.A., in *Issledovaniya prostranstvennykh gazodinamicheskikh techenii na osnove opticheskikh metodov* (Optical Studies of Spatial Gas-dynamic Flows), *Proc. Zhukovskii Air Force Engineering Academy* (Moscow: 1971) p. 121.
25. Vasil'ev L.A., Ershov I.V. *Interferometer s difraktsionnoi reshetkoi* (Diffraction Grating Interferometer) (Moscow: Mashinostroenie, 1997).
26. Vest C.M. *Holographic Interferometry* (New York: Wiley, 1979; Moscow: Mir, 1982).